The CbbQO-type rubisco activases encoded in carboxysome gene clusters can activate carboxysomal form IA rubiscos

Yi-Chin Candace Tsai[‡][iD], Lynette Liew[‡], Zhijun Guo, Di Liu, and Oliver Mueller-Cajar*

From the School of Biological Sciences, Nanyang Technological University, Singapore, Singapore

Edited by Joseph Jez

The CO_2-fixing enzyme rubisco is responsible for almost all carbon fixation. This process frequently requires rubisco activase (Rca) machinery, which couples ATP hydrolysis to the removal of inhibitory sugar phosphates, including the rubisco substrate ribulose 1,5-bisphosphate (RuBP). Rubisco is sometimes compartmentalized in carboxysomes, bacterial microcompartments that enable a carbon dioxide concentrating mechanism (CCM). Characterized carboxysomal rubiscos, however, are not prone to inhibition, and often no activase machinery is associated with these enzymes. Here, we characterize two carboxysomal rubiscos of the form IA^C clade that are associated with CbbQO-type Rcas. These enzymes release RuBP at a much lower rate than the canonical carboxysomal rubisco from *Synechococcus* PCC6301. We found that CbbQO-type Rcas encoded in carboxysome gene clusters can remove RuBP and the tight-binding transition state analog carboxyarabinitol 1,5-bisphosphate from cognate rubiscos. The *Acidithiobacillus ferrooxidans* genome encodes two form IA rubiscos associated with two sets of *cbbQ* and *cbbO* genes. We show that the two CbbQO activase systems display specificity for the rubisco enzyme encoded in the same gene cluster, and this property can be switched by substituting the C-terminal three residues of the large subunit. Our findings indicate that the kinetic and inhibitory properties of proteobacterial form IA rubiscos are diverse and predict that Rcas may be necessary for some α-carboxysomal CCMs. These findings will have implications for efforts aiming to introduce biophysical CCMs into plants and other hosts for improvement of carbon fixation of crops.

The CO_2-fixing enzyme rubisco catalyzes the most quantitatively significant conversion of CO_2 gas to biomass, operating in the majority of autotrophic organisms. All genuine rubiscos possess an ancient and conserved active site architecture and a complex reaction mechanism (1). An inevitable consequence is a side reaction with oxygen (2), leading to the production of the metabolite 2-phosphoglycolate, which must be recycled *via* salvage pathways ("photorespiration") to avoid the loss of carbon from the Calvin cycle (3). It is thought that the emergence of rubisco prior to the oxygenation of earth's atmosphere predisposed the enzyme to display a limited capacity to adapt to modern atmospheric conditions (4, 5). To compensate, diverse clades of rubisco-dependent autotrophs readily and convergently evolved a broad suite of carbon dioxide concentrating mechanisms (CCMs), many of which rely on spatial compartmentation of the carboxylase (6). A solution encountered in all cyanobacteria and many proteobacteria involves sequestration of cellular rubisco in protein-encapsulated microcompartments known as carboxysomes (7–9).

Rubisco requires the cofactors CO_2 and Mg^{2+} to bind at the active site prior to becoming catalytically competent (10). It has recently emerged that most if not all rubiscos are prone to binding of the substrate ribulose 1,5-bisphosphate (RuBP) to the apoenzyme, leading to formation of inhibited complexes of various stability (11, 12). Inhibited rubisco complexes can also form when a suite of other phosphorylated sugars binds to either the apoenzyme or holoenzyme. These include the rubisco "misfire" products xylulose 1,5-bisphosphate (13) and D-glycero-2,3-pentodiulose-1,5-bisphosphate (14) or the nighttime inhibitor in plants: 2-carboxy-D-arabinitol 1-phosphate (15). Inhibited rubisco complexes are recognized and remodeled by a growing suite of diverse molecular chaperones, known as the rubisco activases (Rcas). All the characterized Rca proteins belong to the superfamily of AAA+ ATPases (16, 17) but have been co-opted to the Rca function at least three times independently (11). Rca function involves ATP hydrolysis, which is coupled to rubisco active site rearrangements that release the inhibitory sugars (18).

Proteobacterial genomes frequently encode up to three *bona fide* rubisco enzymes (19–22), which in some cases have been shown to be differentially expressed according to factors such as the environmental CO_2 concentration (23–25). Form I rubiscos encoded in α-carboxysomal gene clusters are referred to as form IA^C, whereas those not associated with carboxysome genes are form IA^Q rubiscos (19). *Acidithiobacillus ferrooxidans* possesses three operons encoding three different rubiscos (25). Each cluster also contains single copies of distinct *cbbQ* and *cbbO* genes. We have previously characterized the gene products of *cbbQ* and *cbbO* found in two clusters (encoding form IA^Q and form II rubiscos) and demonstrated biochemically that CbbQO complexes functionally form a third class of Rca (26). Mechanistically, CbbQO-type Rcas are highly distinct to the other two classes;

---

they belong to the MoxR family of AAA+ proteins (27, 28) and rely on the CbbO adaptor protein for function. CbbO binds rubisco *via* its von Willebrand factor A domain, and a single CbbO subunit binds to the conserved concave surface of the CbbQ hexamer (29).

The *cbbQ* and *cbbO* genes found in the *A. ferrooxidans* carboxysomal cluster (Fig. 1) are therefore likely to encode an Rca that specifically remodels inhibited carboxysomal form IA^C rubiscos. This hypothesis was tested by Sutter *et al.* for *Halothiobacillus neapolitanus*; however, the reported activase assays used purified CbbQ complexes lacking the essential CbbO subunit. Analysis of fractured carboxysomes in that work showed that CbbQ associated with a shell enriched pellet fraction, suggesting an interaction of CbbQ with the carboxysome shell (30, 31).

A caveat regarding the need for carboxysomal Rcas relates to the fact that previously examined carboxylases (belonging to the form IB clade) do not form stably inhibited complexes with the substrate RuBP (32–34). In addition, the frequent absence of candidate Rca genes in the genomes of cyanobacteria and proteobacteria that utilize carboxysomes suggest that Rca function is not strictly required for the carboxysomal CCM (35, 36). The existence of carboxysomal Rca systems will require ATP and ADP to pass the carboxysomal shell, which is widely believed to be selectively permeable and possibly even gated (37). With regard to form IB rubisco, it has very recently been shown that the Rca-like protein found in some cyanobacterial clades (38, 39) is a functional Rca in *Nostoc* sp. PCC7120 (40). Its mechanism involves an interaction with the rubisco large subunit N terminus, which is conserved in the higher plant system (41). The homolog encoded by *Fremyella diplosiphon* showed the expected carboxysomal localization (35).

Recently, there have been tremendous advances toward introducing carboxysomes and their associated rubiscos into higher plants (42, 43). In conjunction with a functional CCM, it is predicted that such a modification could enhance photosynthetic carbon assimilation of a C3 plant by 60% (44, 45). It has even been possible to transfer a powered and functional carboxysome CCM into *Escherichia coli* (46). In order to fully capitalize on these advances, it is imperative to resolve and define the role of Rcas in such compartments.

Here, using pure components, we functionally characterize the properties of rubiscos and define the Rca function of CbbQO complexes encoded in the carboxysomal clusters of *A. ferrooxidans* and *H. neapolitanus*, respectively. We found that both chaperones are indeed capable of removing both loose-binding RuBP and the exceptionally tight-binding transition-state analog carboxy-arabinitol 1,5-bisphosphate (CABP) from form IA^C rubisco active sites. The specificity of the two CbbQO complexes associated with the two form IA rubisco operons in *A. ferrooxidans* can be switched *via* amino acid substitutions in the RbcL C terminus. We propose that carboxysomal rubiscos exist on a continuum related to their kinetic properties and tendencies to bind inhibitors. Their position on the continuum determines the extent of activase dependency and permits activase loss in organisms possessing high-velocity and low-efficiency carboxylases.

Results

Bioinformatics analysis of form IA rubiscos and associated CbbQO sequences

We performed BLAST homology searches using the *A. ferrooxidans* IA^Q large subunit sequence (UniProt: B7JA24) to collect form IA CbbL sequences. The sequences were then classified according to their gene neighborhoods. Form IA^C sequences were followed by *csoS2* and other carboxysome genes and contained *cbbQ* and *cbbO* in the operon. Form IA^Q genes were directly adjacent to *cbbQ* and did not encode carboxysome genes (Fig. 1). Among α-carboxysome clusters encoding form IA^C rubisco and CbbQ and CbbO, there appear to be two arrangements. In one cluster type, *cbbQ* and *cbbO* genes are positioned directly downstream of the shell-encoding genes. In the other cluster type, *cbbO* and *cbbQ* are separated by genes encoding the dab complex (Fig. 1) (47).

We decided to introduce a new form IA^C division: these constituted form IA CbbL sequences encoded in carboxysomal clusters that did not contain *cbbQ* and *cbbO* genes and were designated as IAC_Q$^-$. Form IA^C and IA^Q sequences are all proteobacterial, whereas the IAC_Q$^-$ sequences are also found in α-cyanobacteria and the endosymbiont of *Paulinella chromatophora* (48). A maximum likelihood tree indicated that
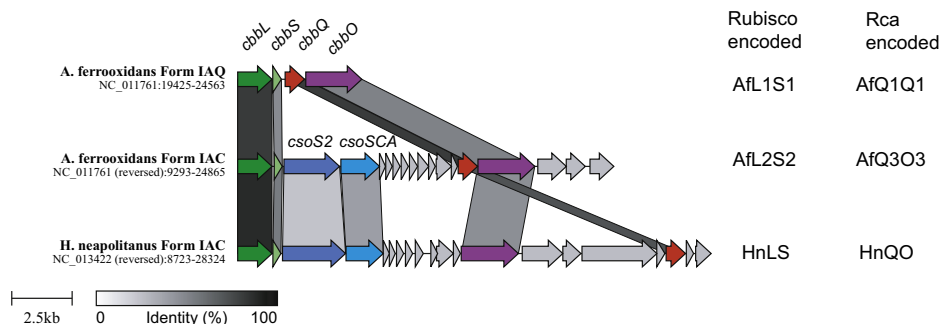
Figure 1. Form I rubisco-associated operons in *Acidithiobacillus ferrooxidans* and *Halothiobacillus neapolitanus*. The relative position and sequence identity between rubisco (*cbbL* and *cbbS*) and activase (*cbbq* and *cbbO*) encoding genes is indicated. The terminology used in this work for the different rubiscos and Rca complexes encoded in the operons is also shown. Rca, rubisco activase.

form IA^C and form IA^Q CbbL sequences do not form distinct clades, as observed previously (19) (Fig. S1*A*). In contrast, form IAC_Q$^-$ large subunits formed a well-supported separate clade. In addition, the multiple sequence alignment (Fig. S2) revealed that all the form IA^C and IA^Q CbbL sequences possessed a C-terminal motif (KLDXXHK or KLDXXXR) consistent with the experimentally characterized CbbQO interaction (26). In contrast, all examined form IAC$^{Q^-}$ sequences had diverse C termini, which generally terminated two residues earlier (KLDXX) (Fig. S2).

The phylogenetic relationship between form IA rubisco-associated CbbS (Fig. S1*B*), CbbQ (Fig. S1*C*), and CbbO (Fig. S1*D*) amino acid sequences could not be used to predict whether they were associated with carboxysomal clusters (IA^C or IA^Q rubiscos). There is therefore no support for distinct ancestral form IA^Q or IA^C rubisco/activase systems. Instead form IA-associated CbbQO activase components appear to change their context over time, which would lead one to expect biochemical compatibility between non-native rubisco–Rca pairs.

The inhibition and reaction kinetics of CbbQO-associated form IA rubiscos are diverse

Existing data suggest that carboxysomal form I rubiscos do not form tight-binding complexes with RuBP in the apo state but readily release the inhibitor. This property correlates with high carboxylation velocities and Michaelis constants for CO_2, but this generalization is exclusively derived from cyanobacterial form IB enzymes (32, 33, 40, 49, 50). It is not known whether carboxysomal form IA^C rubiscos follow the same trend. We therefore decided to compare kinetic parameters and the spontaneous release of RuBP for the different form IA enzymes encoded in *A. ferrooxidans*, the carboxysomal form IA^C rubisco from *H. neapolitanus* and the carboxysomal form IB model enzyme from *Synechococcus* PCC6301. Following purification (Fig. 2*A*), the apoenzymes were preincubated with RuBP to form enzyme–RuBP (ER) (Fig. 2*B*) and subsequently added to a rubisco assay mixture. The activity of the ER complex (*red traces*) was then compared with that of the preactivated Enzyme-CO_2-Mg^{2+} (ECM) holoenzyme (*black traces*) allowing the rate of RuBP release to be estimated by quantifying the formation of active ECM holoenzymes (32, 51) (Fig. 2*B*).

As reported earlier (26, 52, 53), the form IA^Q rubisco (AfL1S1) formed a stable binary complex with RuBP and had the slowest inhibitor release rate (Fig. 2*C*). The three carboxysomal enzymes displayed faster but highly variable reactivation rates (Fig. 2, *D–G*). The activity of fully activated AfL2S2 form IA^C enzyme was not linear over the time course, indicating a loss of functional active sites over the reaction time course (the "fallover" phenomenon commonly observed in higher plant rubiscos (32, 51)). Compared with the very loose RuBP-binding phenotype of the cyanobacterial form IB SynLS rubisco, all form IA enzymes assayed here had much slower RuBP release rates and would therefore be predicted to benefit from an associated activase system.

Kinetic characterization of the form IA enzymes indicated that the two *A. ferrooxidans* rubiscos had highly similar carboxylation velocities (~ 5.5 s^{-1}) and Michaelis constants (40–50 μM) for CO_2 (Table 1 and Fig. S3). The carboxysomal AfL2S2 form IA^C enzyme had a much reduced specificity factor of 32, compared with 56 for the form IA^Q rubisco. *H. neapolitanus* form IA^C (HnLS) rubisco kinetics were distinct, being faster and possessing a much higher Michaelis constant for CO_2. Compared with the fast model carboxysomal form IB Synechococcus enzyme SynLS (54–56), HnLS displayed an intermediate phenotype (Table 1).

The observed general trend of increased carboxylation velocities and reduced specificity factors for the carboxysomal enzymes is commonly observed for rubiscos that are supplied by CCMs. However, the three carboxysomal enzymes characterized here possessed a significant diversity in their kinetics. For the four enzymes evaluated here, there was a clear correlation between RuBP release rate and both the K_m (CO_2) and carboxylation turnover rate (Fig. 2, *H* and *I*). This observation is consistent with the hypothesis by Tcherkez *et al.* (57), which predicts that inhibitor binding should be enhanced in rubiscos that display high affinities for CO_2 and the associated low carboxylation velocities.

The small selection of kinetic data and inhibitory properties shown here and reported in the literature (42, 52, 53, 58–61) suggest that the form IA clade of rubiscos are likely to have diverse kinetics related to the relative ability of host organisms to acquire and concentrate CO_2.

The CbbQO complexes encoded in carboxysome clusters are functional Rcas

Sutter *et al.* (30) demonstrated that the CbbQ protein encoded by the *H. neapolitanus* carboxysomal gene cluster physically associated with the α-carboxysome. Consistent with the requirement for association of the adaptor protein CbbO (26), in that study, the CbbQ hexamer was not able to activate inhibited carboxysomal rubisco. To clarify the function of the CbbQ and CbbO isoforms encoded by carboxysome gene clusters, we produced in *E. coli* and purified the form IA rubisco-associated CbbQO complexes encoded by *A. ferrooxidans* (IA^Q-AfQ1O1 and IA^C-AfQ3O3) and *H. neapolitanus* IA^C (HnQO) (Fig. 3*A*). The ATPase activity of the purified AfQ3O3 complex was similar to that of the AfQ1O1 complex. HnQO was much faster, showing an ATPase activity of ~ 8 min^{-1}/CbbQ protomer (Fig. 3*B*).

We then assayed carboxysomal AfQ3O3 for the ability to remove the transition state analog CABP from the *A. ferrooxidans* form IA^C (AfL2S2) holoenzyme (ECM), using conditions previously established for the *A. ferrooxidans* form IA^Q enzyme (26) (Fig. 3*C*). AfQ3O3 was almost nonfunctional, but increasing the concentration of the crowding agent PEG 3350 from 5% to 13% v/v resulted in an eightfold activity increase and thus robust Rca function (Fig. 3, *D* and *F*). The dependence of AfQ3O3 on high PEG concentrations was seen irrespective whether ECM component (ECMC) or ER (Fig. 3*E*) was used as inhibited rubisco, or whether the assays were
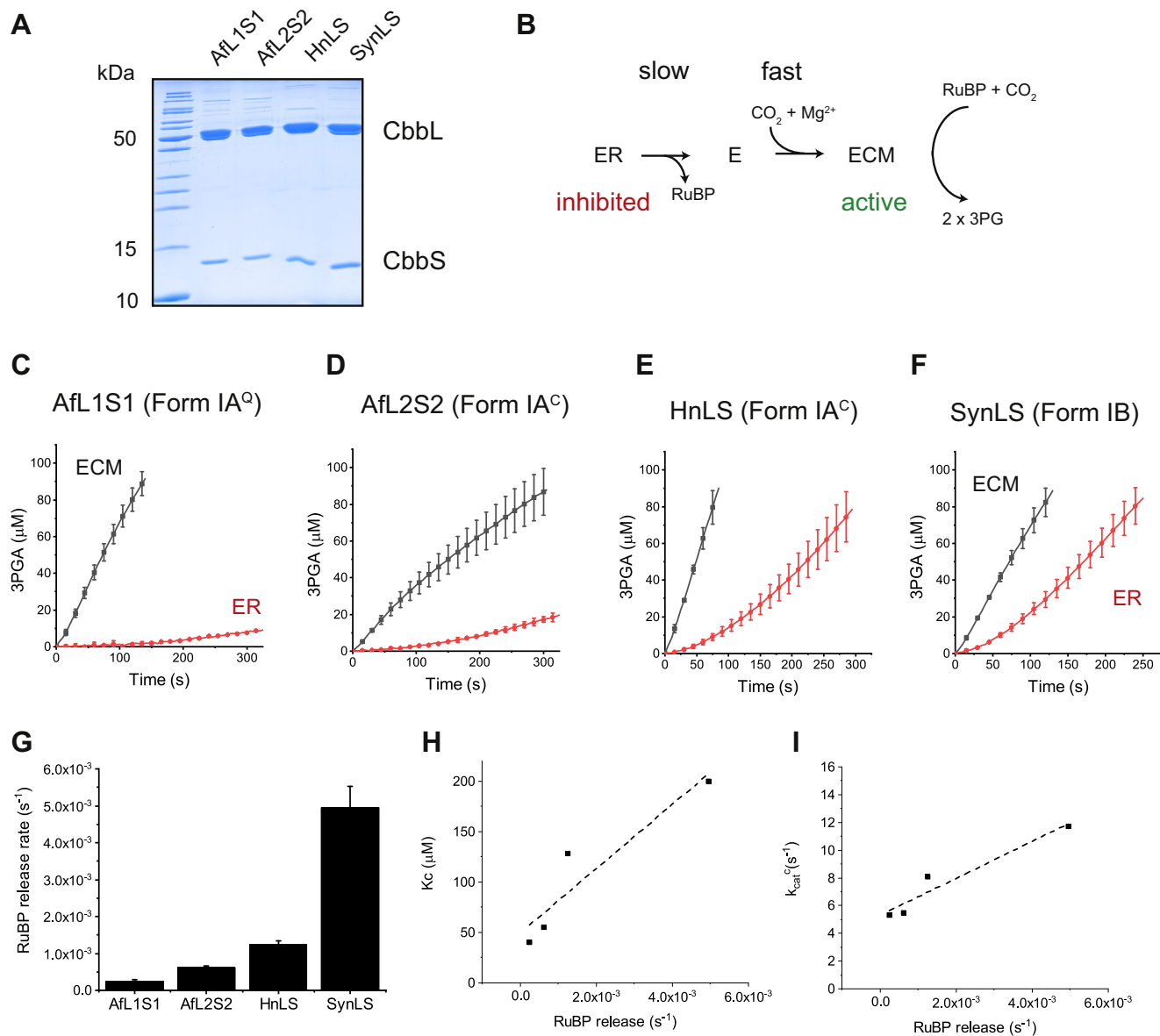
Figure 2. CbbQO-associated form IA rubiscos possess diverse inhibitory properties. *A*, SDS-PAGE analysis of purified rubiscos. *B*, scheme describing the relationship between inactive enzyme–RuBP (ER) complex and the active (ECM) holoenzyme. *C–F*, inhibitor release kinetics of different form I enzymes is variable. Carboxylation time courses of 0.1 μM of fully activated holoenzyme (ECM) or apo-rubisco–RuBP (ER) complex are shown (50 mM NaHCO$_3$ and 1 mM RuBP). Error bars signify mean and standard deviation of three technical replicates. *G*, the RuBP release rate was derived from the ER time courses shown in *C–F*. *H* and *I*, scatterplot of RuBP release rate against K_m (CO$_2$) (*H*) and carboxylation rate (*I*) for the four enzymes. ECM, Enzyme-CO$_2$-Mg^{2+}; RuBP, ribulose 1,5-bisphosphate.

performed in the presence of 5 or 20 mM bicarbonate (Fig. 3*F*). AfQ3O3 is therefore the activase of the carboxysomal AfL2S2 (form IA^C) rubisco, which is encoded in the same operon (Fig. 1*A*).

Table 1
Kinetic parameters of the form I rubiscos

Rubisco	k_{cat}^c (s^{-1})	K_C (μM)	k_{cat}^c/K_C $(s^{-1}.mM^{-1})$	$S_{C/O}$
AfL1S1	5.2 ± 0.1	40 ± 3	130	56.4 ± 1.7
AfL2S2	5.5 ± 0.1	55 ± 3	100	32.2 ± 0.5
HnLS	8.0 ± 0.4	127 ± 16	63	43.6 ± 1.1
SynLS[a]	11.7 ± 0.6	200 ± 4	59	42.7 ± 2.8

Michaelis–Menten plots used to derive the parameters are shown in Fig. S3.
[a] Data from the study by Davidi *et al.* (56).

HnQO was able to remove CABP from its cognate form IA^C rubisco HnLS even in the absence of PEG (Fig. 3*G*), although inclusion of the polymer also greatly enhanced Rca activity (Fig. 3, *G–I*). Titrating both HnQO and PEG concentrations in this assay demonstrated a concentration dependence for both components and showed that Rca function was similar at 0.8 μM HnQO/13% PEG and 3.2 μM HnQO/5% PEG (concentration expressed as CbbQ protomer) (Fig. S4). This finding is consistent with the dominant volume exclusion contribution of macromolecular crowding. Here, the crowding agent occupies a substantial fraction of the volume, and this results in a smaller available volume for both rubisco and activase, leading to higher biochemical activities (62–64). The strong positive

Figure 3. Carboxysomal CbbQO-type rubisco activases are functional. *A*, SDS-PAGE analysis of purified CbbQO activases. *B*, ATPase activity of the CbbQO complexes expressed per protomer CbbQ. *C*, experimental scheme of the rubisco activase assays. Apo-rubisco (E) is activated using the non-substrate CO_2 and Mg^{2+} cofactors to form ECM. The transition-state analog CABP stoichiometrically binds to ECM to form inactive ECMC. Addition of a compatible CbbQO activase and ATP releases CABP to recover ECM, which produces 3PG in the spectrophotometric assay. Inhibited carboxysomal rubiscos (0.3 μM ECMC [*D*] or ER [*E*] active sites) from *Acidithiobacillus ferrooxidans* were assayed at 20 mM $NaHCO_3$ in the absence and presence of the cognate CbbQO activase AfQ3O3 (0.27 μM oligomer). *F*, quantified Rca activities of AfQ3O3 using inhibited carboxysomal *A. ferrooxidans* rubisco. *G* and *H*, activation time courses of *Halothiobacillus neapolitanus* rubisco in the presence and absence of HnQO using the same conditions as in *D* and *E*. *I*, activation of *H. neapolitanus* rubisco by different CbbQO activases at 5 and 13% v/v PEG (20 mM $NaHCO_3$). Error bars indicate mean and standard deviation of three technical replicates. CABP, carboxy-arabinitol 1,5-bisphosphate; ECM, Enzyme-CO_2-Mg^{2+}; ECMC, ECM-CABP; Rca, rubisco activase.

effect of molecular crowding presumably relates to the carboxysomal microenvironment of AfL2S2 and HnLS. This property may be related to carboxysomal rubisco's coacervation with the multivalent rubisco linker protein CsoS2 (65, 66). A strong positive effect of PEG is also observed when assaying green-type plant Rcas, which are found in the crowded chloroplast stroma (67, 68).

The two Rca complexes from *A. ferrooxidans* (AfQ3O3 and AfQ1O1) were also able to remove CABP from HnLS but displayed much lower activities in combination with a great dependence on high PEG concentrations (Fig. 3*I*).

These data establish that the gene products of *cbbQ* and *cbbO* encoded by carboxysomal gene clusters in both *A. ferrooxidans* and *H. neapolitanus* are capable of reactivating inhibited carboxysomal form IA^C rubisco complexes. The function of the *A. ferrooxidans* activase was greatly enhanced by high concentrations of the molecular crowding agent PEG.

The role of the RbcL C terminus in recognition by CbbQO

The RbcL C terminus is critical for CbbQO-mediated activation for both form I and form II rubiscos. The interaction is

mediated by a C-terminal HK/R motif, and modification of the C terminus (including single-residue truncations and extensions) eliminates the ability of rubisco to become activated by CbbQO (26) (Fig. 4A). Carboxysomal rubisco large subunits that do not encode *cbbQ* and *cbbO* in the operon (FormIAC_Q⁻) are missing this motif and generally have a shorter C-terminal motif KLDXX. In contrast, when cbbQ and cbbO are present in the operon, the large subunit C-terminal motif is longer (KLDXXHK or KLDXXXR) (Figs. 4B and S2).

The form IA^C rubiscos from *A. ferrooxidans* and *H. neapolitanus* do not possess the conserved HK/R motif but instead encode an alternative "NR" C terminus (Fig. 4C). Two AfL2S2 rubisco C-terminal variants were produced and purified (Fig. 4D) and displayed similar carboxylation kinetics and spontaneous RuBP release under our assay conditions (Figs. 4E and S5). This permitted us to compare their activation kinetics using the two *A. ferrooxidans* CbbQO complexes AfQ1O1 and AfQ3O3.

Activation of the form IA^C AfL2S2 rubisco by either AfQ1O1 or AfQ3O3 was poor at 5% v/v PEG (Fig. 4, F and H). Substituting N472 with histidine or replacing the last three amino acids (VNR to AHK) resulted in a sixfold enhancement in AfQ1O1 activase function (Fig. 4, F and H). This indicates that the mutations significantly enhanced the low affinity of AfQ1O1 for the carboxysomal rubisco.

This dramatic increase in function was not observed when using the cognate AfQ3O3 assayed at 13% v/v PEG (Fig. 4G). Whereas AfL2S2N472H permitted a 30% increase in AfQ3O3 function compared with the wildtype AfL2S2, AfL2S2 (AHK) showed a ∼60% reduction in activation rate (Fig. 4, G and H). Substituting the last three residues of the C terminus therefore resulted in a specificity switch regarding the preference of the two *A. ferrooxidans* CbbQO complexes (Fig. 4I).

These results suggest that the as yet unidentified binding sites of *A. ferrooxidans* Q1O1 and Q3O3 to the RbcL C terminus are nonequivalent and can enable the activases to discriminate between substrate rubiscos. However, for both activases, a histidine residue at the penultimate position of RbcL is preferred to achieve high activase functionality *in vitro*. A crowded environment like the one found in a carboxysome may relax the requirement for a high rubisco–Rca binding affinity.

Discussion

In this contribution, we conclusively demonstrate that CbbQO complexes encoded in proteobacterial carboxysomal operons are functional at removing inhibitory sugar phosphates from carboxysomal form IA^C rubisco active sites. The widespread evolutionary conservation of these genes, in conjunction with the functional green-type activase from *Nostoc* (40), therefore suggests that robust carboxysome CCM function relies on the ability to remove RuBP or other sugar phosphates from the rubisco active site in some bacteria. Our work does not inform on the nature of the physiological inhibitor(s), but these are likely to be reaction misfire products, such as xylulose 1,5-bisphosphate or possibly

pentadiulose-1,5 bisphosphate (12, 13). Elucidation of this issue will necessitate a detailed biochemical study of rubiscos isolated from bacterial mutants with lesions in the associated *cbbq/cbbO* genes. RuBP is unlikely to be a relevant inhibitor because the concentration of Mg^{2+} and CO_2 is expected to remain high in the carboxysome, which will disfavor decarbamylation and ER formation.

A. ferrooxidans possesses two form IA rubiscos, one form II enzyme and three CbbQO complexes (26, 56). Its form IA^C rubisco (AfL2S2) presents with a similar k_{cat}^c and K_m (CO_2) but a reduced specificity factor compared with the form IA^Q enzyme (AfL1S1) (Table 1). The tendency of AfL2S2 to spontaneously release RuBP from the apoenzyme is less than that of the other carboxysomal rubiscos tested but more rapid than the form IA^Q rubisco AfL1S1 (Fig. 2). Our work thus shows that three carboxysomal rubiscos possess highly variable carboxylase kinetics and inhibitor binding. A well-characterized parallel regarding kinetics is the situation in pyrenoid-containing diatoms, where a wide variety of kinetic constants are also observed and interpreted to relate to relative CCM strength (69). A stronger CCM will permit the selection pressure on K_m (CO_2) and $S_{c/o}$ to relax, and this will permit higher carboxylase velocities (57, 70). These properties may be related to the relative availability of metabolic energy and inorganic carbon for these organisms, which will determine the CO_2 concentrations that can be achieved at the carboxysomal rubisco active site. It is possible that *H. neapolitanus* and cyanobacterial rubiscos experience higher CO_2 concentrations because their metabolic modes (sulfur oxidation and oxygenic photosynthesis) generate copious amounts of energy. In contrast, *A. ferrooxidans* grows at low pH, which translates to an absence of the bicarbonate pool, and uses the energetically challenging iron-oxidizing metabolism (25). Its carboxysomal rubisco may thus be exposed to lower CO_2 levels.

Our findings also show that in *A. ferrooxidans*, the CbbQO complexes are specific for the form IA rubisco encoded in their gene cluster, and that this specificity is dependent on the identity of the RbcL C terminus, which has been implicated in CbbQO function previously (26) (Fig. 4). This biochemical finding implies that in *A. ferrooxidans*, it will be important to package the correct (AfL2S2) rubisco in the carboxysome together with its AfQ3O3 activase. Recent discoveries elucidating the mechanisms of α-carboxysomal rubisco compartmentalization *via* the CsoS2 rubisco linker protein provide a straightforward experimental framework to explore these issues (65, 71).

The requirement for activase-mediated rubisco remodeling in carboxysome function has been controversial (30, 35), and in particular, the presence of *cbbQ* and *cbbO* in carboxysomal gene clusters has remained unexplained (45, 72).

In light of our findings, we propose that dependence of organisms bearing carboxysome CCMs on activase function will vary and relate to both phylogenetic history and to a continuum of kinetic and inhibitory properties of the associated carboxylases. These properties are sculpted by the
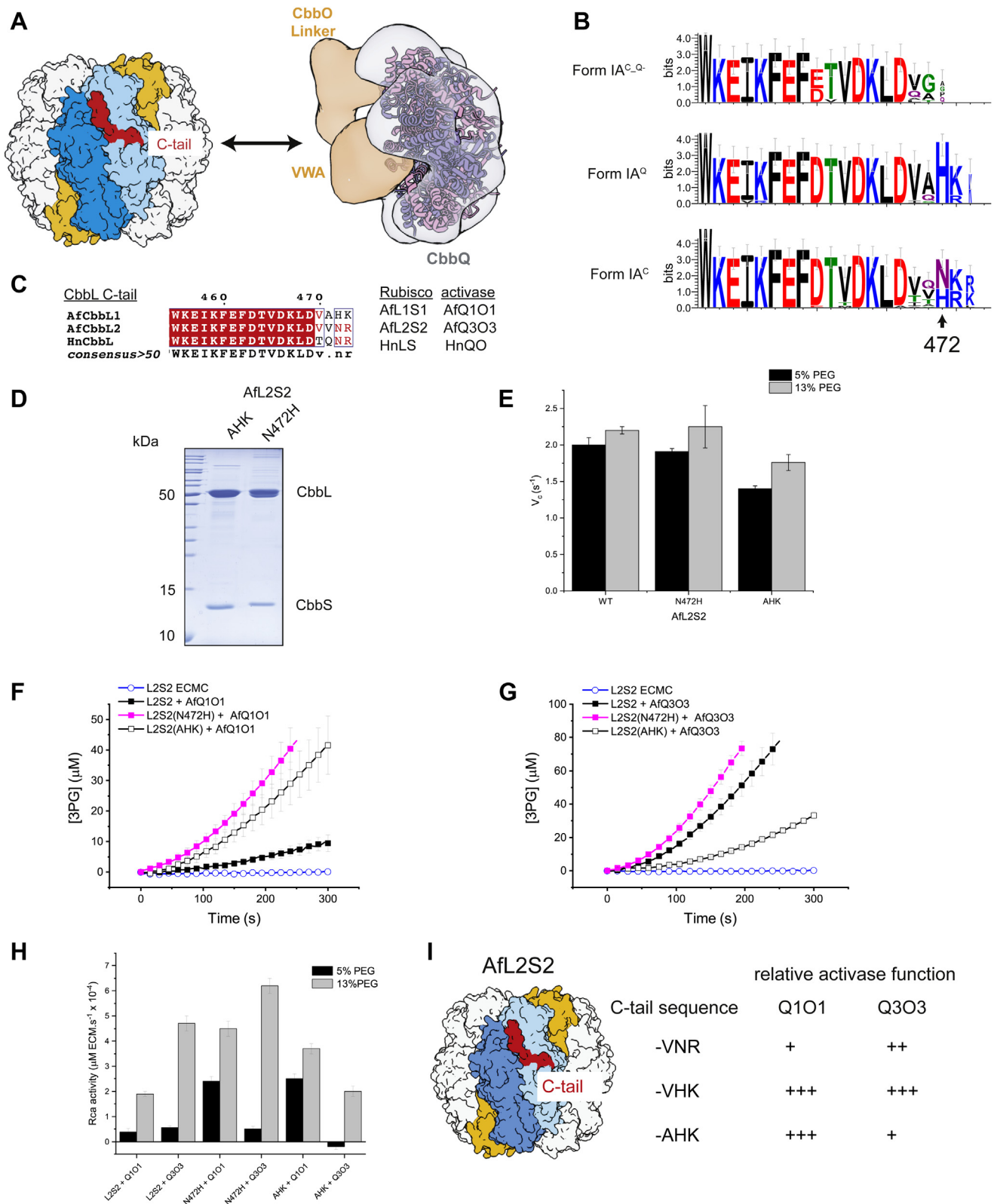
Figure 4. The RbcL C terminus encodes Rca specificity. *A*, model of CbbQO function. The large subunit C terminus (*red*) is required for interaction with the activase and likely interacts with the CbbO adaptor protein. *B*, Logo motifs of the C termini generated from the RbcL sequences used for the phylogenetic tree in Fig. S1. *C*, alignment of the form IA RbcL C termini used in this study. *D*, SDS-PAGE analysis of purified AfL2S2 variants. AHK: the VNR C terminus is substituted with AHK. *E*, carboxylase activity of fully activated (ECM) AfL2S2 wildtype and variant proteins assayed at 20 mM NaHCO₃. *F*, mutation at the C terminus of AfL2S2 enhances activation of ECMC complexes by Q1O1 (5% v/v PEG and 20 mM NaHCO₃). *G*, the N472H mutation enhances AfQ3O3 function, whereas the AHK substitution reduces it (13% v/v PEG and 20 mM NaHCO₃). *H*, quantified Rca activities for AfL2S2 and its variants. *I*, scheme summarizing how mutations of the RbcL C tail influence activase function. Rca, rubisco activase.

prevailing CO_2 concentrations experienced by the active sites during evolution (59, 69). On one extreme of the spectrum, there are carboxysomal rubiscos, such as the *A. ferrooxidans* form IA^C enzyme (AfL2S2), which do not readily release RuBP from the apoenzyme, and are only modestly faster than the cytoplasmic form IA^Q enzymes (AfL1S1). Such carboxysomal enzymes will be predicted to strictly coexist with Rca-encoding genes. At the other extreme of the continuum, the majority of cyanobacteria do not encode Rca homologs. Consistently, the fast Synechococcus form IB enzyme rapidly dissociates from inhibitory RuBP and XuBP (32). However, its K_m (CO_2) is exceptionally high, and concordantly, the carboxylase efficiency k_{cat}^C/K_C is poor.

The enzyme from *H. neapolitanus* is intermediate to the extreme examples. Inhibitory compounds are released more readily, the enzyme is fast and possesses a high K_m (CO_2) but not as exaggerated as the cyanobacterial rubisco. In addition, experimental results suggest that deleting CbbQ or CbbO has a negligible effect on fitness under laboratory conditions (47). It is possible that a fitness defect would become apparent if growth under energy-limited conditions was explored (73). Transferring the *H. neapolitanus* carboxysomal genes and other CCM components into *E. coli* was successful, even if CbbQ was nonfunctional (46). It is possible that in this scenario, the fitness defect is too subtle to be detected in the context tested in the laboratory.

Although the outlined physiological data suggest that the *H. neapolitanus* CbbQO activase is not critical, here, we show that biochemically the system is functional. In addition, in our bioinformatics analysis of CbbL sequences, we did not encounter IAC_Q$^-$ branches inside the form IA^C/A^Q cluster (Fig. S1). Evolutionary loss of the CbbQO activase system thus appears to be a rare event. Finally, an article published during revision of this article compared *E. coli*-produced *H. neapolitanus* carboxysomes. It was found that if HnQO was incorporated, the carboxysomes were more functional at fixing CO_2 in the presence of substoichiometric amounts of CABP (74).

Further systematic characterization of carboxysomal rubisco kinetics, their inhibitory properties, and activase dependencies will contribute to our appreciation of the carboxylase intrinsic tradeoffs (57, 75–77). It is likely that biotechnological exploitation of carboxysomes in plants and other organisms will benefit from taking into account a comprehensive understanding of these factors.

Experimental procedures

Bioinformatics analysis

BLAST searches were performed using the AfCbbL1 sequence (UniProt: B7JA24) to query the Integrated Microbial Genome database (78) and the National Center for Biotechnology Information. Classification into form IA^Q, IA^C, and IAC_Q$^-$ was performed manually by inspecting the gene neighborhood of the selected genes. Maximum likelihood phylogenetic trees were constructed using MegaX (www. megasoftware.net) (79) and visualized using iTOL (https://

itol.embl.de) (80). Positions containing gaps or missing data were eliminated. The sequences used are provided in Dataset S1. Multiple sequence alignments were drawn using ESPript (https://espript.ibcp.fr) (81). Gene neighborhoods were visualized using clinker (https://github.com/gamcil/clinker) (82).

Molecular biology

Rubisco- and activase-encoding genes were amplified from genomic DNA of *H. neapolitanus* ATCC23641 and *A. ferrooxidans* ATCC23270. The *H. neapolitanus cbbL* (Hneap_0922) and *cbbS* (Hneap_0921) genes including the intergenic region were cloned between NdeI and HindIII sites of pET30b to yield pET30b*HnLS*. The carboxysome CbbQO-encoding genes *HncbbQ* (Hneap_0905)/*AfcbbQ3* (AFE_1678) and *HncbbO* (Hneap_0910)/*AfcbbO3* (AFE_1677) were cloned into pHue and pBad33 in the same context as pHue*AfCbbQ1* and pBad33*UbAfcbbO1* (26).

Site-directed mutagenesis was used to introduce mutations into the *AfcbbL2* C terminus. The corresponding primers and plasmids used in this study are listed in Tables S1 and S2. Protein-encoding sequences were verified using DNA sequencing.

Proteins

Proteobacterial rubiscos were produced in *E. coli* BL21(DE3) cells transformed with the appropriate plasmid and purified using anion exchange chromatography followed by size-exclusion chromatography as described for AfL1S1 (26). The SynLS purification protocol was described (55).

Rca complexes were produced in *E. coli* BL21(DE3) harboring the appropriate plasmids (Table S2) and purified using a combination of affinity chromatography, ion exchange chromatography, and size-exclusion chromatography. The purification of AfQ1O1 was described previously (26). AfQ3O3 and HnQO were obtained using the same strategy except that the ion exchange chromatography step was omitted for AfQ3O3. Protein concentrations were quantified using the Bradford assay using bovine serum albumin as the standard.

Enzymatic assays

All assays were performed at 25 °C. ATPase activity was measured using a coupled spectrophotometric assay (83). The CbbQO concentration used was 0.27 μM oligomer. RuBP was synthesized from ribose 5-phosphate and purified by anion exchange chromatography (84, 85). Rubisco and Rca assays were performed using the coupled spectrophotometric rubisco assay (26, 86) and quantified as described (87). ECM holoenzyme was obtained by incubating rubisco (10 μM active sites) in 20 mM Tris–HCl, pH 8.0, 50 mM NaCl, 50 mM NaHCO$_3$, and 10 mM MgCl$_2$ for 10 min at 25 °C. A fourfold molar excess of carboxypentitol bisphosphate (synthesized from RuBP following Ref. (88)) was added to ECM to form ECMC. Excess ligand was then removed by buffer exchange into 20 mM Tris–HCl, pH 8.0, and 50 mM NaCl using Micro-Bio-Spin 6 (BioRad) chromatography columns.

Inhibited ER complex (10 µM) was obtained by incubating apo-rubisco in 20 mM Tris–HCl (pH 8.0), 50 mM NaCl, and 4 mM EDTA for 10 min, followed by addition of RuBP to a final concentration of 0.4 mM for 30 min at 25 °C. Rca assays contained either 5 or 13% v/v PEG 3350 (Sigma–Aldrich).

Rubisco kinetics were determined using radiometric rubisco assays (89). $^{14}CO_2$ fixation assays (0.5 ml of reaction volume) were performed at 25 °C in 7.7 ml septum-capped glass scintillation vials with assay buffer (100 mM *N*-(2-hyroxyethyl)piperazine-*N'*-(3-propanesulfonic acid)–NaOH, pH 8.0, 20 mM $MgCl_2$, and 1 mM EDTA), 10 mg/ml carbonic anhydrase, and 1 mm RuBP. All the assay components were equilibrated with nitrogen gas prior to addition of $^{14}CO_2$ varying from 2 to 40 mM $NaH^{14}CO_3$ (corresponding to 30–500 µM $^{14}CO_2$). Purified rubisco (~5 µM active sites) was first activated using assay buffer containing 30 mM $NaHCO_3$, and the assay was then initiated by addition of 20 µl of activated rubisco. The assay was stopped after 2 min using 200 µl of 50% (v/v) formic acid. The specific activity of $^{14}CO_2$ was measured using the highest $^{14}CO_2$ concentration and 5.2 nmol of RuBP. The reaction was stopped after 30 min, and the activity was ~220 CPM/nmol RuBP. Active site concentrations were determined using ^{14}C-CABP binding assays (90). CO_2/O_2 specificity assays were performed as described (89, 91). The reactions were equilibrated in a defined gas mixture (999,300 ppm O_2; 700 ppm CO_2; Air Liquide Singapore Private Limited) prior to the addition of [1-^3H]-RuBP.

Data availability

All data are contained within the article and supporting information.

Abbreviations—The abbreviations used are: CABP, carboxy-arabinitol 1,5-bisphosphate; CCM, carbon dioxide concentrating mechanism; ECM, Enzyme-CO_2-Mg^{2+}; ECMC, ECM-CABP; ER, enzyme–RuBP; MOE, Ministry of Education; NRF, National Research Foundation; Rca, rubisco activase; RuBP, ribulose 1,5-bisphosphate.

References

1. Cleland, W. W., Andrews, T. J., Gutteridge, S., Hartman, F. C., and Lorimer, G. H. (1998) Mechanism of rubisco - the carbamate as general base. *Chem. Rev.* **98**, 549–561
2. Tcherkez, G. (2016) The mechanism of rubisco-catalysed oxygenation. *Plant Cell Environ.* **39**, 983–997
3. Walker, B. J., VanLoocke, A., Bernacchi, C. J., and Ort, D. R. (2016) The costs of photorespiration to food production now and in the future. *Annu. Rev. Plant Biol.* **67**, 107–129
4. Whitney, S. M., Houtz, R. L., and Alonso, H. (2011) Advancing our understanding and capacity to engineer nature's CO(2)-sequestering enzyme, rubisco. *Plant Physiol.* **155**, 27–35
5. Liu, D., Ramya, R. C. S., and Mueller-Cajar, O. (2017) Surveying the expanding prokaryotic rubisco multiverse. *FEMS Microbiol. Lett.* **364**, 16
6. Erb, T. J., and Zarzycki, J. (2018) A short history of RubisCO: The rise and fall (?) of nature's predominant CO2 fixing enzyme. *Curr. Opin. Biotechnol.* **49**, 100–107
7. Rae, B. D., Long, B. M., Badger, M. R., and Price, G. D. (2013) Functions, compositions, and evolution of the two types of carboxysomes: Polyhedral microcompartments that facilitate CO2 fixation in cyanobacteria and some proteobacteria. *Microbiol. Mol. Biol. Rev.* **77**, 357–379
8. Kerfeld, C. A., and Melnicki, M. R. (2016) Assembly, function and evolution of cyanobacterial carboxysomes. *Curr. Opin. Plant Biol.* **31**, 66–75
9. Borden, J. S., and Savage, D. F. (2021) New discoveries expand possibilities for carboxysome engineering. *Curr. Opin. Microbiol.* **61**, 58–66
10. Lorimer, G. H., Badger, M. R., and Andrews, T. J. (1976) The activation of ribulose-1,5-bisphosphate carboxylase by carbon dioxide and magnesium ions. Equilibria, kinetics, a suggested mechanism and physiological implications. *Biochemistry* **15**, 529–536
11. Mueller-Cajar, O. (2017) The diverse AAA+ machines that repair inhibited rubisco active sites. *Front. Mol. Biosci.* **4**, 31
12. Parry, M. A. J., Keys, A. J., Madgwick, P. J., Carmo-Silva, A. E., and Andralojc, P. J. (2008) Rubisco regulation: A role for inhibitors. *J. Exp. Bot.* **59**, 1569–1580
13. Bracher, A., Sharma, A., Starling-Windhof, A., Hartl, F. U., and Hayer-Hartl, M. (2015) Degradation of potent rubisco inhibitor by selective sugar phosphatase. *Nat. Plants* **1**, 14002
14. Kim, K., and Portis, A. R. (2004) Oxygen-dependent H2O2 production by rubisco. *FEBS Lett.* **571**, 124–128
15. Andralojc, P. J., Madgwick, P. J., Tao, Y., Keys, A., Ward, J. L., Beale, M. H., Loveland, J. E., Jackson, P. J., Willis, A. C., Gutteridge, S., and Parry, M. A. J. (2012) 2-Carboxy-D-arabinitol 1-phosphate (CA1P) phosphatase: Evidence for a wider role in plant rubisco regulation. *Biochem. J.* **442**, 733–742
16. Hanson, P. I., and Whiteheart, S. W. (2005) AAA+ proteins: Have engine, will work. *Nat. Rev. Mol. Cell Biol.* **6**, 519–529
17. Puchades, C., Sandate, C. R., and Lander, G. C. (2020) The molecular principles governing the activity and functional diversity of AAA+ proteins. *Nat. Rev. Mol. Cell Biol.* **21**, 43–58
18. Bhat, J. Y., Thieulin-Pardo, G., Hartl, F. U., and Hayer-Hartl, M. (2017) Rubisco activases: AAA+ chaperones adapted to enzyme repair. *Front. Mol. Biosci.* **4**, 20
19. Badger, M. R., and Bek, E. J. (2008) Multiple rubisco forms in proteobacteria: Their functional significance in relation to CO2 acquisition by the CBB cycle. *J. Exp. Bot.* **59**, 1525–1541
20. Scott, K. M., Williams, J., Porter, C. M. B., Russel, S., Harmer, T. L., Paul, J. H., Antonen, K. M., Bridges, M. K., Camper, G. J., Campla, C. K., Casella, L. G., Chase, E., Conrad, J. W., Cruz, M. C., Dunlap, D. S., *et al.* (2018) Genomes of ubiquitous marine and hypersaline Hydrogenovibrio, Thiomicrorhabdus and Thiomicrospira spp. encode a diversity of mechanisms to sustain chemolithoautotrophy in heterogeneous environments. *Environ. Microbiol.* **20**, 2686–2708

21. Tourova, T. P., Spiridonova, E. M., Berg, I. A., Kuznetsov, B. B., and Sorokin, D. Y. (2006) Occurrence, phylogeny and evolution of ribulose-1,5-bisphosphate carboxylase/oxygenase genes in obligately chemolithoautotrophic sulfur-oxidizing bacteria of the genera Thiomicrospira and Thioalkalimicrobium. *Microbiology (Reading)* **152**, 2159–2169

22. Tabita, F. R. (1999) Microbial ribulose 1,5-bisphosphate carboxylase/oxygenase: A different perspective. *Photosynth. Res.* **60**, 1–28

23. Toyoda, K., Ishii, M., and Arai, H. (2018) Function of three RuBisCO enzymes under different CO2 conditions in Hydrogenovibrio marinus. *J. Biosci. Bioeng.* **126**, 730–735

24. Yoshizawa, Y., Toyoda, K., Arai, H., Ishii, M., and Igarashi, Y. (2004) CO2-responsive expression and gene organization of three ribulose-1,5-bisphosphate carboxylase/oxygenase enzymes and carboxysomes in hydrogenovibrio marinus strain MH-110. *J. Bacteriol.* **186**, 5685–5691

25. Esparza, M., Jedlicki, E., Gonzalez, C., Dopson, M., and Holmes, D. S. (2019) Effect of CO2 concentration on uptake and assimilation of inorganic carbon in the extreme acidophile Acidithiobacillus ferrooxidans. *Front. Microbiol.* **10**, 603

26. Tsai, Y. C., Lapina, M. C., Bhushan, S., and Mueller-Cajar, O. (2015) Identification and characterization of multiple rubisco activases in chemoautotrophic bacteria. *Nat. Commun.* **6**, 8883

27. Snider, J., and Houry, W. A. (2006) MoxR AAA+ ATPases: A novel family of molecular chaperones? *J. Struct. Biol.* **156**, 200–209

28. Wong, K. S., and Houry, W. A. (2012) Novel structural and functional insights into the MoxR family of AAA+ ATPases. *J. Struct. Biol.* **179**, 211–221

29. Tsai, Y. C., Ye, F., Liew, L., Liu, D., Bhushan, S., Gao, Y. G., and Mueller-Cajar, O. (2020) Insights into the mechanism and regulation of the CbbQO-type rubisco activase, a MoxR AAA+ ATPase. *Proc. Natl. Acad. Sci. U. S. A.* **117**, 381–387

30. Sutter, M., Roberts, E. W., Gonzalez, R. C., Bates, C., Dawoud, S., Landry, K., Cannon, G. C., Heinhorst, S., and Kerfeld, C. A. (2015) Structural characterization of a newly identified component of alpha-carboxysomes: The AAA+ domain protein CsoCbbQ. *Sci. Rep.* **5**, 16243

31. Heinhorst, S., and Cannon, G. C. (2020) Bacterial microcompartments. In: Jendrossek, D., ed. *Bacterial Organelles and Organelle-like Inclusions*, Springer International Publishing, Cham: 125–147

32. Pearce, F. G. (2006) Catalytic by-product formation and ligand binding by ribulose bisphosphate carboxylases from different phylogenies. *Biochem. J.* **399**, 525–534

33. Andrews, T. J., and Abel, K. M. (1981) Kinetics and subunit interactions of ribulose bisphosphate carboxylase-oxygenase from the cyanobacterium, Synechococcus sp. *J. Biol. Chem.* **256**, 8445–8451

34. Lee, B. G., Read, B. A., and Tabita, F. R. (1991) Catalytic properties of recombinant octameric, hexadecameric, and heterologous cyanobacterial/bacterial ribulose-1,5-bisphosphate carboxylase oxygenase. *Arch. Biochem. Biophys.* **291**, 263–269

35. Lechno-Yossef, S., Rohnke, B. A., Belza, A. C. O., Melnicki, M. R., Montgomery, B. L., and Kerfeld, C. A. (2020) Cyanobacterial carboxysomes contain a unique rubisco-activase-like protein. *New Phytol.* **225**, 793–806

36. Zarzycki, J., Axen, S. D., Kinney, J. N., and Kerfeld, C. A. (2013) Cyanobacterial-based approaches to improving photosynthesis in plants. *J. Exp. Bot.* **64**, 787–798

37. Sommer, M., Sutter, M., Gupta, S., Kirst, H., Turmo, A., Lechno-Yossef, S., Burton, R. L., Saechao, C., Sloan, N. B., Cheng, X., Chan, L. G., Petzold, C. J., Fuentes-Cabrera, M., Ralston, C. Y., and Kerfeld, C. A. (2019) Heterohexamers formed by CcmK3 and CcmK4 increase the complexity of beta carboxysome shells. *Plant Physiol.* **179**, 156–167

38. Li, L.-A., Zianni, M., and Tabita, F. R. (1999) Inactivation of the monocistronic rca gene in Anabaena variabilis suggests a physiological ribulose bisphosphate carboxylase/oxygenase activase-like function in heterocystous cyanobacteria. *Plant Mol. Biol.* **40**, 467–478

39. Li, L. A., Gibson, J. L., and Tabita, F. R. (1993) The rubisco activase (Rca) gene is located downstream from Rbcs in Anabaena sp strain Ca and is detected in other Anabaena Nostoc strains. *Plant Mol. Biol.* **21**, 753–764

40. Flecken, M., Wang, H., Popilka, L., Hartl, F. U., Bracher, A., and Hayer-Hartl, M. (2020) Dual functions of a rubisco activase in metabolic repair and recruitment to carboxysomes. *Cell* **183**, 457–473.e20

41. Ng, J., Guo, Z., and Mueller-Cajar, O. (2020) Rubisco activase requires residues in the large subunit N-terminus to remodel inhibited plant rubisco. *J. Biol. Chem.* **295**, 16427–16435

42. Long, B. M., Hee, W. Y., Sharwood, R. E., Rae, B. D., Kaines, S., Lim, Y. L., Nguyen, N. D., Massey, B., Bala, S., von Caemmerer, S., Badger, M. R., and Price, G. D. (2018) Carboxysome encapsulation of the CO2-fixing enzyme rubisco in tobacco chloroplasts. *Nat. Commun.* **9**, 3570

43. Lin, M. T., Occhialini, A., Andralojc, P. J., Parry, M. A., and Hanson, M. R. (2014) A faster rubisco with potential to increase photosynthesis in crops. *Nature* **513**, 547–550

44. McGrath, J. M., and Long, S. P. (2014) Can the cyanobacterial carbon-concentrating mechanism increase photosynthesis in crop species? A theoretical analysis. *Plant Physiol.* **164**, 2247–2261

45. Rae, B. D., Long, B. M., Forster, B., Nguyen, N. D., Velanis, C. N., Atkinson, N., Hee, W. Y., Mukherjee, B., Price, G. D., and McCormick, A. J. (2017) Progress and challenges of engineering a biophysical carbon dioxide-concentrating mechanism into higher plants. *J. Exp. Bot.* **68**, 3717–3737

46. Flamholz, A. I., Dugan, E., Blikstad, C., Gleizer, S., Ben-Nissan, R., Amram, S., Antonovsky, N., Ravishankar, S., Noor, E., Bar-Even, A., Milo, R., and Savage, D. F. (2020) Functional reconstitution of a bacterial CO2 concentrating mechanism in Escherichia coli. *Elife* **9**, e59882

47. Desmarais, J. J., Flamholz, A. I., Blikstad, C., Dugan, E. J., Laughlin, T. G., Oltrogge, L. M., Chen, A. W., Wetmore, K., Diamond, S., Wang, J. Y., and Savage, D. F. (2019) DABs are inorganic carbon pumps found throughout prokaryotic phyla. *Nat. Microbiol.* **4**, 2204–2215

48. Marin, B., Nowack, E. C., Glockner, G., and Melkonian, M. (2007) The ancestor of the Paulinella chromatophore obtained a carboxysomal operon by horizontal gene transfer from a nitrococcus-like gamma-proteobacterium. *BMC Evol. Biol.* **7**, 85

49. Read, B. A., and Tabita, F. R. (1994) High substrate specificity factor ribulose bisphosphate carboxylase/oxygenase from eukaryotic marine algae and properties of recombinant cyanobacterial rubisco containing "algal" residue modifications. *Arch. Biochem. Biophys.* **312**, 210–218

50. Li, L. A., and Tabita, F. R. (1997) Maximum activity of recombinant ribulose 1,5-bisphosphate carboxylase/oxygenase of *Anabaena* sp. strain CA requires the product of the *rbcX* gene. *J. Bacteriol.* **179**, 3793–3796

51. Pearce, F. G., and Andrews, T. J. (2003) The relationship between side reactions and slow inhibition of ribulose-bisphosphate carboxylase revealed by a loop 6 mutant of the tobacco enzyme. *J. Biol. Chem.* **278**, 32526–32536

52. Hernandez, J. M., Baker, S. H., Lorbach, S. C., Shively, J. M., and Tabita, F. R. (1996) Deduced amino acid sequence, functional expression, and unique enzymatic properties of the form I and form II ribulose bisphosphate carboxylase oxygenase from the chemoautotrophic bacterium Thiobacillus denitrificans. *J. Bacteriol.* **178**, 347–356

53. Horken, K. M., and Tabita, F. R. (1999) The "green" form I ribulose 1,5-bisphosphate carboxylase/oxygenase from the nonsulfur purple bacterium rhodobacter capsulatus. *J. Bacteriol.* **181**, 3935–3941

54. Morell, M. K., Paul, K., O'Shea, N. J., Kane, H. J., and Andrews, T. J. (1994) Mutations of an active site threonyl residue promote β elimination and other side reactions of the enediol intermediate of the ribulosebisphosphate carboxylase reaction. *J. Biol. Chem.* **269**, 8091–8098

55. Mueller-Cajar, O., and Whitney, S. M. (2008) Evolving improved Synechococcus Rubisco functional expression in Escherichia coli. *Biochem. J.* **414**, 205–214

56. Davidi, D., Shamshoum, M., Guo, Z., Bar-On, Y. M., Prywes, N., Oz, A., Jablonska, J., Flamholz, A., Wernick, D. G., Antonovsky, N., de Pins, B., Shachar, L., Hochhauser, D., Peleg, Y., Albeck, S., *et al.* (2020) Highly active rubiscos discovered by systematic interrogation of natural sequence diversity. *EMBO J.* **39**, e104081

57. Tcherkez, G. G. B., Farquhar, G. D., and Andrews, T. J. (2006) Despite slow catalysis and confused substrate specificity, all ribulose bisphosphate carboxylases may be nearly perfectly optimized. *Proc. Natl. Acad. Sci. U. S. A.* **103**, 7246–7251

58. Viale, A. M., Kobayashi, H., and Akazawa, T. (1990) Distinct properties of Escherichia coli products of plant-type ribulose-1,5-bisphosphate carboxylase/oxygenase directed by two sets of genes from the photosynthetic bacterium Chromatium-vinosum. *J. Biol. Chem.* **265**, 18386–18392

59. Shih, P. M., Occhialini, A., Cameron, J. C., Andralojc, P. J., Parry, M. A., and Kerfeld, C. A. (2016) Biochemical characterization of predicted Precambrian RuBisCO. *Nat. Commun.* **7**, 10382

60. Jordan, D. B., and Chollet, R. (1985) Subunit dissociation and reconstitution of ribulose-1,5-bisphosphate carboxylase from Chromatium-vinosum. *Arch. Biochem. Biophys.* **236**, 487–496

61. Hayashi, N. R., Oguni, A., Yaguchi, T., Chung, S. Y., Nishihara, H., Kodama, T., and Igarashi, Y. (1998) Different properties of gene products of three sets ribulose 1,5-bisphosphate carboxylase/oxygenase from a marine obligately autotrophic hydrogen-oxidizing bacterium, Hydrogenovibrio marinus strain MH-110. *J. Ferment. Bioeng.* **85**, 150–155

62. Zhou, H.-X., Rivas, G., and Minton, A. P. (2008) Macromolecular crowding and confinement: Biochemical, biophysical, and potential physiological consequences. *Annu. Rev. Biophys.* **37**, 375–397

63. Rivas, G., and Minton, A. P. (2016) Macromolecular crowding in vitro, in vivo, and in between. *Trends Biochem. Sci.* **41**, 970–981

64. Ellis, R. J. (2001) Macromolecular crowding: Obvious but underappreciated. *Trends Biochem. Sci.* **26**, 597–604

65. Oltrogge, L. M., Chaijarasphong, T., Chen, A. W., Bolin, E. R., Marqusee, S., and Savage, D. F. (2020) Multivalent interactions between CsoS2 and rubisco mediate alpha-carboxysome formation. *Nat. Struct. Mol. Biol.* **27**, 281–287

66. Cai, F., Dou, Z., Bernstein, S. L., Leverenz, R., Williams, E. B., Heinhorst, S., Shively, J., Cannon, G. C., and Kerfeld, C. A. (2015) Advances in understanding carboxysome assembly in Prochlorococcus and Synechococcus implicate CsoS2 as a critical component. *Life (Basel)* **5**, 1141–1171

67. Salvucci, M. E. (1992) Subunit interactions of rubisco activase - polyethylene-glycol promotes self-association, stimulates atpase and activation activities, and enhances interactions with rubisco. *Arch. Biochem. Biophys.* **298**, 688–696

68. Shivhare, D., and Mueller-Cajar, O. (2017) In vitro characterization of thermostable CAM rubisco activase reveals a rubisco interacting surface loop. *Plant Physiol.* **174**, 1505–1516

69. Young, J. N., Heureux, A. M., Sharwood, R. E., Rickaby, R. E., Morel, F. M., and Whitney, S. M. (2016) Large variation in the rubisco kinetics of diatoms reveals diversity among their carbon-concentrating mechanisms. *J. Exp. Bot.* **67**, 3445–3456

70. Iniguez, C., Capo-Bauca, S., Niinemets, U., Stoll, H., Aguilo-Nicolau, P., and Galmes, J. (2020) Evolutionary trends in RuBisCO kinetics and their co-evolution with CO2 concentrating mechanisms. *Plant J.* **101**, 897–918

71. Wunder, T., and Mueller-Cajar, O. (2020) Biomolecular condensates in photosynthesis and metabolism. *Curr. Opin. Plant Biol.* **58**, 1–7

72. Kerfeld, C. A., Aussignargues, C., Zarzycki, J., Cai, F., and Sutter, M. (2018) Bacterial microcompartments. *Nat. Rev. Microbiol.* **16**, 277–290

73. Holthuijzen, Y. A., van Dissel-Emiliani, F. F. M., Kuenen, J. G., and Konings, W. N. (1987) Energetic aspects of CO2 uptake in Thiobacillus neapolitanus. *Arch. Microbiol.* **147**, 285–290

74. Chen, T., Fang, Y., Jiang, Q., Dykes, G. F., Lin, Y., Price, G. D., Long, B. M., and Liu, L.-N. (2021) Incorporation of functional rubisco activases into engineered carboxysomes to enhance carbon fixation. *ACS Synth. Biol.* https://doi.org/10.1021/acssynbio.1c00311

75. Flamholz, A. I., Prywes, N., Moran, U., Davidi, D., Bar-On, Y. M., Oltrogge, L. M., Alves, R., Savage, D., and Milo, R. (2019) Revisiting trade-offs between rubisco kinetic parameters. *Biochemistry* **58**, 3365–3376

76. Savir, Y., Noor, E., Milo, R., and Tlusty, T. (2010) Cross-species analysis traces adaptation of rubisco toward optimality in a low-dimensional landscape. *Proc. Natl. Acad. Sci. U. S. A.* **107**, 3475–3480

77. Bouvier, J. W., Emms, D. M., Rhodes, T., Bolton, J. S., Brasnett, A., Eddershaw, A., Nielsen, J. R., Unitt, A., Whitney, S. M., and Kelly, S. (2021) Rubisco adaptation is more limited by phylogenetic constraint than by catalytic trade-off. *Mol. Biol. Evol.* **38**, 2880–2896

78. Chen, I. A., Chu, K., Palaniappan, K., Ratner, A., Huang, J., Huntemann, M., Hajek, P., Ritter, S., Varghese, N., Seshadri, R., Roux, S., Woyke, T., Eloe-Fadrosh, E. A., Ivanova, N. N., and Kyrpides, N. C. (2021) The IMG/M data management and analysis system v.6.0: New tools and advanced capabilities. *Nucleic Acids Res.* **49**, D751–D763

79. Kumar, S., Stecher, G., Li, M., Knyaz, C., and Tamura, K. (2018) Mega X: Molecular evolutionary genetics analysis across computing platforms. *Mol. Biol. Evol.* **35**, 1547–1549

80. Letunic, I., and Bork, P. (2021) Interactive tree of life (iTOL) v5: An online tool for phylogenetic tree display and annotation. *Nucleic Acids Res.* **49**, W293–W296

81. Gouet, P., Courcelle, E., Stuart, D. I., and Metoz, F. (1999) ESPript: Analysis of multiple sequence alignments in PostScript. *Bioinformatics* **15**, 305–308

82. Gilchrist, C. L. M., and Chooi, Y. H. (2021) Clinker & clustermap.js: Automatic generation of gene cluster comparison figures. *Bioinformatics*. https://doi.org/10.1093/bioinformatics/btab007

83. Stotz, M., Mueller-Cajar, O., Ciniawsky, S., Wendler, P., Hartl, F. U., Bracher, A., and Hayer-Hartl, M. (2011) Structure of green-type rubisco activase from tobacco. *Nat. Struct. Mol. Biol.* **18**, 1366–U1378

84. Horecker, B. L., Hurwitz, J., and Weissbach, A. (1958) Ribulose diphosphate. *Biochem. Prep.* **6**, 83–90

85. Kane, H. J., Wilkin, J. M., Portis, A. R., and Andrews, T. J. (1998) Potent inhibition of ribulose-bisphosphate carboxylase by an oxidized impurity in ribulose-1,5-bisphosphate. *Plant Physiol.* **117**, 1059–1069

86. Lan, Y., and Mott, K. A. (1991) Determination of apparent Km values for ribulose 1,5-bisphosphate carboxylase oxygenase (rubisco) activase using the spectrophotometric assay of rubisco activity. *Plant Physiol.* **95**, 604–609

87. Loganathan, N., Tsai, Y.-C. C., and Mueller-Cajar, O. (2016) Characterization of the heterooligomeric red-type rubisco activase from red algae. *Proc. Natl. Acad. Sci. U. S. A.* **113**, 14019–14024

88. Pierce, J., Tolbert, N. E., and Barker, R. (1980) Interaction of ribulosebisphosphate carboxylase-oxygenase with transition-state analogs. *Biochemistry* **19**, 934–942

89. Wilson, R. H., Martin-Avila, E., Conlan, C., and Whitney, S. M. (2018) An improved Escherichia coli screen for rubisco identifies a protein-protein interface that can enhance CO2-fixation kinetics. *J. Biol. Chem.* **293**, 18–27

90. Kubien, D. S., Brown, C. M., and Kane, H. J. (2011) Quantifying the amount and activity of rubisco in leaves. *Methods Mol. Biol.* **684**, 349–362

91. Kane, H. J., Viil, J., Entsch, B., Paul, K., Morell, M. K., and Andrews, T. J. (1994) An improved method for measuring the CO2/O2 specificity of ribulosebisphosphate carboxylase-oxygenase. *Aust. J. Plant Physiol.* **21**, 449–461

92. Wunder, T., Cheng, S. L. H., Lai, S. K., Li, H. Y., and Mueller-Cajar, O. (2018) The phase separation underlying the pyrenoid-based microalgal Rubisco supercharger. *Nat. Commun.* **9**, 5076